A heme-degradation pathway in a blood-sucking insect

Gabriela O. Paiva-Silva*†, Christine Cruz-Oliveira*†, Ernesto S. Nakayasu‡§, Clarissa M. Maya-Monteiro¶, Boris C. Dunkov‖, Hatisaburo Masuda*, Igor C. Almeida‡§**, and Pedro L. Oliveira*††

*Instituto de Bioquímica Médica, Programa de Biologia Molecular e Biotecnologia, Universidade Federal do Rio de Janeiro, CEP 21941-590, Rio de Janeiro, Brazil; ‡Department of Biological Sciences, University of Texas, El Paso, TX 79968-0519; §Departamento de Parasitologia, Universidade de São Paulo, São Paulo, SP 05508-900, Brazil; ¶Departamento de Fisiologia e Farmacodinâmica, Instituto Oswaldo Cruz, RJ, 21045-900, Rio de Janeiro, Brazil; and ‖Department of Biochemistry and Molecular Biophysics, Center for Insect Science, University of Arizona, Tucson, AZ 85721

Communicated by John H. Law, University of Georgia, Athens, GA, March 17, 2006 (received for review January 9, 2006)

Hematophagous insects are vectors of diseases that affect hundreds of millions of people worldwide. A common physiological event in the life of these insects is the hydrolysis of host hemoglobin in the digestive tract, leading to a massive release of heme, a known prooxidant molecule. Diverse organisms, from bacteria to plants, express the enzyme heme oxygenase, which catalyzes the oxidative degradation of heme to biliverdin (BV) IX, CO, and iron. Here, we show that the kissing bug *Rhodnius prolixus*, a vector of Chagas' disease, has a unique heme-degradation pathway wherein heme is first modified by addition of two cysteinylglycine residues before cleavage of the porphyrin ring, followed by trimming of the dipeptides. Furthermore, in contrast to most known heme oxygenases, which generate BV IXα, in this insect, the end product of heme detoxification is a dicysteinyl-BV IXγ. Based on these results, we propose a heme metabolizing pathway that includes the identified intermediates produced during modification and cleavage of the heme porphyrin ring.

biliverdin | heme oxygenase | oxidative stress | *Rhodnius*

Heme is a ubiquitous molecule that is involved in many essential biological processes, including oxygen transport, respiration, photosynthesis, drug detoxification, and signal transduction (1). However, free heme is a potent prooxidant, leading to the formation of reactive oxygen species that can damage a variety of biological molecules (2). Furthermore, heme can associate with phospholipid membranes, altering bilayer structure and, thus, causing cell disruption (3, 4). For this reason, the cells strictly regulate heme homeostasis. An important component of this control is heme oxygenase (HO), an enzyme that is expressed by organisms as diverse as bacteria and plants (5–7). Heme degradation by HO proceeds by a multistep mechanism that involves rapid hydroxylation at one of the meso-carbons of the porphyrin ring, the α-meso-carbon in most of the organisms, oxygen-dependent elimination of the hydroxylated meso-carbon as CO-producing verdoheme, and oxidative cleavage of verdoheme to biliverdin (BV) IX in a reaction that depends on reducing equivalents and O_2, with concomitant release of Fe^{2+} (6–9). This heme-degradation pathway has been extensively studied in the last decade, not only for its role in heme detoxification and iron recycling (2), but also because the cleavage products of the porphyrin ring, BV and CO, play important physiological roles (10). In mammals, CO, a gaseous messenger, has antiinflammatory (11) and antiapoptotic (12) effects, and it is clear that BV and its reduced product bilirubin may function as important antioxidants (13–16). Moreover, in algae, cyanobacteria, and higher plants, BV is a precursor for the synthesis of essential chromophores (17).

BVs and their derivatives, associated with different proteins, are found in the hemolymph and integument of insects of different orders (18), providing camouflage, especially for larvae feeding on plants. However, in hematophagous insects, heme degradation has been overlooked, despite the fact that these insects undoubtedly have to deal with one of the highest dietary heme concentrations in nature. These animals face an intense oxidative stress condition upon degradation of host hemoglobin during digestion. Thus, in the course of evolution, these animals have developed an array of strategies to counteract heme cytotoxicity to adapt successfully to blood feeding (19–22).

Here, we have investigated heme degradation in the bloodsucking bug *Rhodnius prolixus*, the vector of *Trypanosoma cruzi*, the etiologic agent of Chagas' disease, or American trypanosomiasis. We show that, in contrast to all other organisms studied to date, heme breakdown follows a complex pathway, with four distinct intermediates, and results in dicysteinyl-BV IXγ as the end product.

Results

BV Production in *R. prolixus*. The heart of the bloodsucking bug *R. prolixus* is green in color because of the accumulation of pigment in the pericardial cells (Fig. 1*A*). This pigment, also observed in midgut cells (Fig. 1*B*), was assumed to be identical to BV (23). Although the midgut would have been an obvious choice to study heme degradation in a bloodfeeding animal, we decided to perform most of the experiments with the insect heart, because the presence of large amounts of heme in the gut presented experimental difficulties, especially concerning the HPLC separation of some heme metabolites that are described below. To investigate whether the green pigment was produced from heme degradation, we injected female insects with [^{14}C]heme bound to RHBP, a *R. prolixus* heme-binding protein that can transport heme to many tissues, including the heart (24). Reverse-phase HPLC analysis of heart homogenates (Fig. 1*C*) revealed a single major radioactive peak that shows a light-absorption spectrum typical of BV, with λmax at 360 nm and 689 nm (Fig. 1*D*). However, this *R. prolixus* BV (RpBV) was eluted with a more hydrophilic retention time than BV IXα, the canonical product of heme degradation catalyzed by HO (Fig. 1*C*), suggesting the existence of structural differences between RpBV and BV IXα. The same result was also obtained from the analysis of midgut homogenates (data not shown). Furthermore, injecting heme into the hemocoel induced accumulation of RpBV in the pericardial cells *in vivo*, a process that was inhibited by coinjecting

Conflict of interest statement: No conflicts declared.

Abbreviations: BV, biliverdin; ESI, electrospray ionization; HO, heme oxygenase; RpBV, *R. prolixus* BV; SnPP IX, Sn-protoporphyrin IX.

†G.O.P.-S. and C.C.-O. contributed equally to this work.

**To whom correspondence may be addressed at: Department of Biological Sciences, University of Texas, 500 West University Avenue, El Paso, TX 79968-0519. E-mail: icalmeida@utep.edu.

††To whom correspondence may be addressed at: Instituto de Bioquímica Médica, Programa de Biologia Molecular e Biotecnologia, Universidade Federal do Rio de Janeiro, CCS, Sala 5 Bloco D subsolo, Ilha do Fundão, 21941-590, Rio de Janeiro, Brazil. E-mail: pedro@bioqmed.ufrj.br.

www.pnas.org/cgi/doi/10.1073/pnas.0602224103

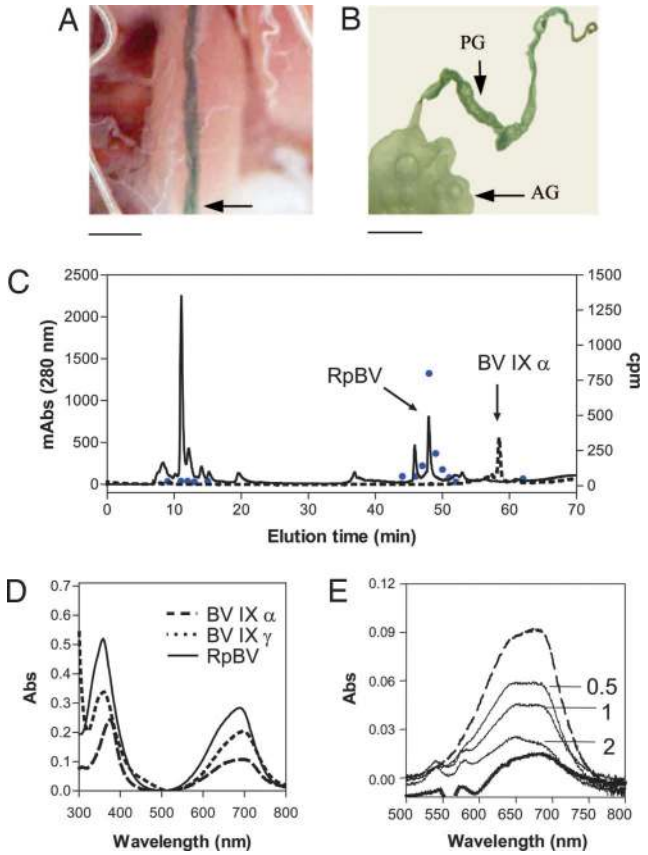

Fig. 1. *In vivo* heme degradation by *R. prolixus*. (*A*) Dorsal side of a dissected *R. prolixus* abdomen, showing the green heart (arrow). (*B*) Green *R. prolixus* midgut 30 days after blood meal, when digestion is completed. AG, anterior midgut; PG, posterior midgut. (*C*) Reverse-phase HPLC profile of heart homogenate from [^{14}C]heme-injected insects (solid line). The radioactivity associated with each fraction is indicated by blue dots. The elution profile of BV IXα is shown by a dashed line. (*D*) Light-absorption spectra of BV IXα (dashed line), BV IXγ (dotted line), and purified *R. prolixus* BV, RpBV (solid line). (*E*) Light-absorption spectra of heart homogenates, showing changes in the RpBV content after different treatments: PBS-injected control (thick solid line); insects injected with 10 nmol of heme (dashed line); insects coinjected with 10 nmol of heme and 0.5, 1, and 2 nmol of SnPP IX, as indicated (thin solid lines). [Scale bars, 0.5 mm (*A*) and 0.3 cm (*B*).]

Sn-protoporphyrin IX (SnPP IX), a classical inhibitor of HO (Fig. 1*E*).

Electrospray ionization (ESI)-MS analysis revealed that the purified RpBV has a molecular mass of 824.2 Da ([RpBV + H]$^+$ at m/z 825.2 and [RpBV + 2H]$^{2+}$ at m/z 413.1), higher than that of BV IXα ([BV IXα + H]$^+$ at m/z 583.2) (Fig. 2*A*). Analysis of sequential fragmentation by tandem ESI-MS indicated that RpBV produced a major ion species of m/z 704 by the loss of a residue of 121 Da (Fig. 2*B*). A RpBV daughter-ion species with the same molecular mass as BV IXα (m/z 583.2) was generated by fragmentation of the m/z 704 ion species, again by removal of 121 Da (Fig. 2*B*). These results demonstrated that RpBV comprises BV coupled to two residues of 121 Da. Fragmentation of both the RpBV ion species of m/z 122 and a cysteine standard produced almost identical daughter-ion species (Fig. 2*C*), suggesting that the 121-Da residues coupled to BV were most likely cysteine residues.

Most of the described heme oxygenases hydroxylate heme at the α-meso-carbon position, producing exclusively BV IXα (6–9). Recently, two exceptions were reported: the *Pseudomonas aeruginosa* HO, capable of degrading heme to both δ and β isomers of BV (25), and the recombinant *Drosophila melanogaster* HO, which produced simultaneously δ, β, and α BV isomers *in vitro* (26). Because it is well established that some insects produce BV IXγ (18), we investigated the possibility that RpBV is also the γ isomer. Fragmentation of BV IXγ and the

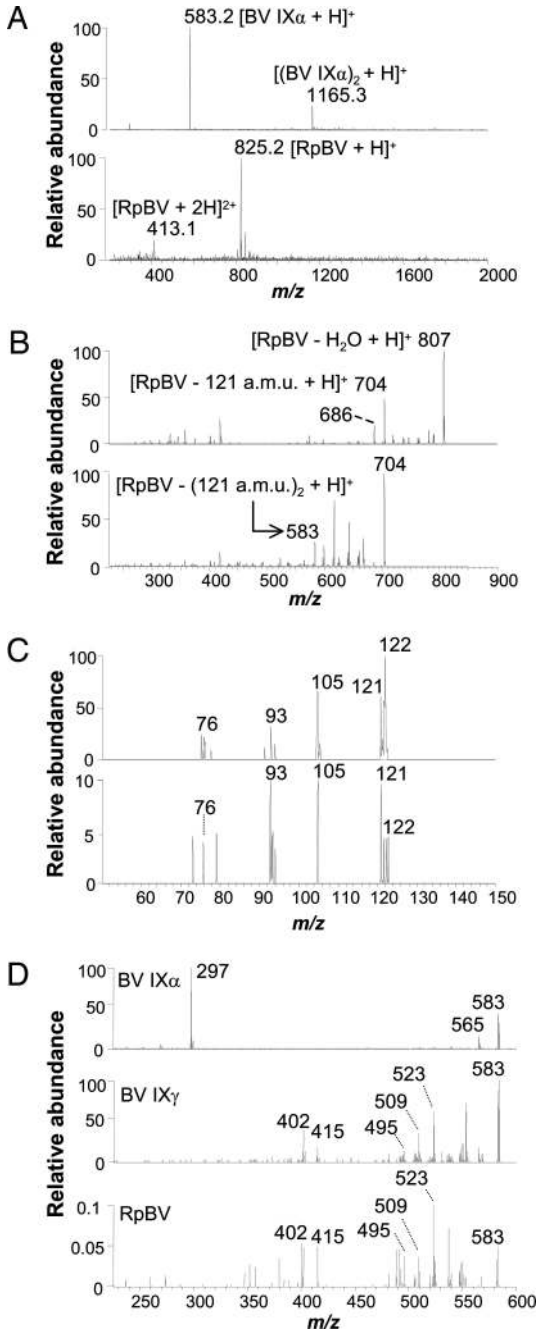

Fig. 2. ESI-MS analysis of the RpBV structure. (*A*) Mass spectra of BV IXα\{[M + H]$^+$ and [2M + H]$^+$ at m/z 583.2 and 1165.3, respectively (*Upper*)\}, and of purified RpBV, indicating a molecular mass of 824.3 Da \{[M + H]$^+$ and [M + 2H]$^{2+}$ at m/z 825.2 and 413.1, respectively (*Lower*)\}. (*B*) Fragmentation (tandem ESI-MS) spectra of RpBV, showing daughter-ion species at m/z 704 (*Upper*), which, by further fragmentation (MS^3), gave origin to a daughter-ion species with the same molecular mass as BV IXα (m/z 583) (*Lower*). a.m.u., atomic mass unit. (*C*) Fragmentation patterns of authentic cysteine (*Upper*) and the ion species at m/z 122 produced by cone fragmentation of RpBV (*Lower*). (*D*) Identification of the RpBV isomer. Fragmentation patterns of BV IXα (*Top*), BV IXγ (*Middle*), and RpBV (*Bottom*) are shown.

RpBV ion species at m/z 583 produced identical daughter-ion species (Fig. 2*D*). This fragmentation pattern was clearly distinct from that obtained by fragmentation of BV IXα (Fig. 2*D*). In support of this finding, the light-absorption spectrum of RpBV, indeed, closely resembled that of BV IXγ (Fig. 1*D*). These results indicate the existence in *R. prolixus* of heme-degrading activity with distinct regiospecificity, capable of cleaving the porphyrin ring at the γ-meso-position.

Taken together, our results clearly demonstrate that the product of the heme-degradation pathway in *R. prolixus* is BV IXγ conjugated to two cysteine residues. To investigate how the two cysteine residues were attached to BV IXγ, we produced chemical modifications of the potentially free amino, carboxyl, and thiol groups of the RpBV cysteine residues by acetylation, methylation, and alkylation reactions, respectively (Fig. 5, which is published as supporting information on the PNAS web site). As expected, BV IXγ (m/z 583.3) was not modified after acetylation, because it has no free amino groups (Fig. 5*A*). In contrast, the acetylation product of RpBV was an ion species at m/z 909.5 (Fig. 5*B*), which corresponds to the addition of one acetyl group (42 Da) to each free amino group of the two cysteine residues, demonstrating that these amino groups are free, thus not involved in the binding of cysteine to BV. Methylation of one and two carboxyl groups of the propionate side chains of BV IXγ produced the ion species at m/z 597.4 and m/z 611.4, respectively (Fig. 5*C*). Methylation of RpBV produced ion species containing three (m/z 867.5) or four (m/z 881.5) modifications, indicating that, in RpBV, a total of four carboxyl groups are available for methylation (two from the BV propionate residues and two from the cysteine residues) (Fig. 5*D*). These results indicate that neither the cysteine carboxyl groups nor the carboxyl groups of BV propionyl side chains are involved in the attachment of the two cysteine residues to BV. Alkylation reactions that should have modified free SH groups did not affect RpBV (Fig. 5*E*), demonstrating that the cysteine thiol groups were involved in the binding of the amino acids to BV.

Our results clearly indicated that the cysteine residues were attached to the vinyl side chains of BV IXγ by thioether bonds (Fig. 5*F*). Thioether linkage may involve the internal (α) carbon atom of the vinyl, as in the attachment of heme to the cysteine residues of *c*-type cytochromes (27). However, based on present evidence we cannot exclude a cysteine sulfur atom binding to the terminal (β) carbon atom of heme vinyl groups. In fact, β-thioether linkage with vinyl group of pyrroles have been identified in bacteriophytochromes (28).

Identification of Heme-Degradation Pathway Intermediates. To determine whether the addition of cysteine occurred before or after the cleavage of the porphyrin ring, female insects were coinjected with heme and SnPP IX. Homogenates of insect hearts were then analyzed by HPLC, and two peaks showed substantial increase, when compared with controls (Fig. 3*A*). Interestingly, the light-absorption spectra of these peaks displayed typical heme Soret bands (Fig. 3*A Inset*). However, as observed for RpBV, these compounds were more hydrophilic than heme, suggesting that they could be modified heme intermediates of the heme-degradation pathway produced before the oxidative cleavage of the porphyrin ring. To test this hypothesis, purified intermediates were analyzed by tandem ESI-MS for structure determination. The most hydrophilic compound, intermediate 2 (Int 2), showed a major singly charged ion species at m/z 972.2, whereas intermediate 1 (Int 1), eluting closer to heme, showed a major singly charged ion species at m/z 794.2 (Fig. 3*B*). Sequential fragmentation of both intermediates by tandem ESI-MS produced an ion species at m/z 776 (Fig. 6 *A* and *B*, which is published as supporting information on the PNAS web site), which, after further fragmentation, generated an ion species at m/z 616 (Fig. 3*C Upper*). This species, in turn, generated daughter species identical to an authentic heme (Fig. 3 *C* and *D*), confirming that these intermediates were modified heme products.

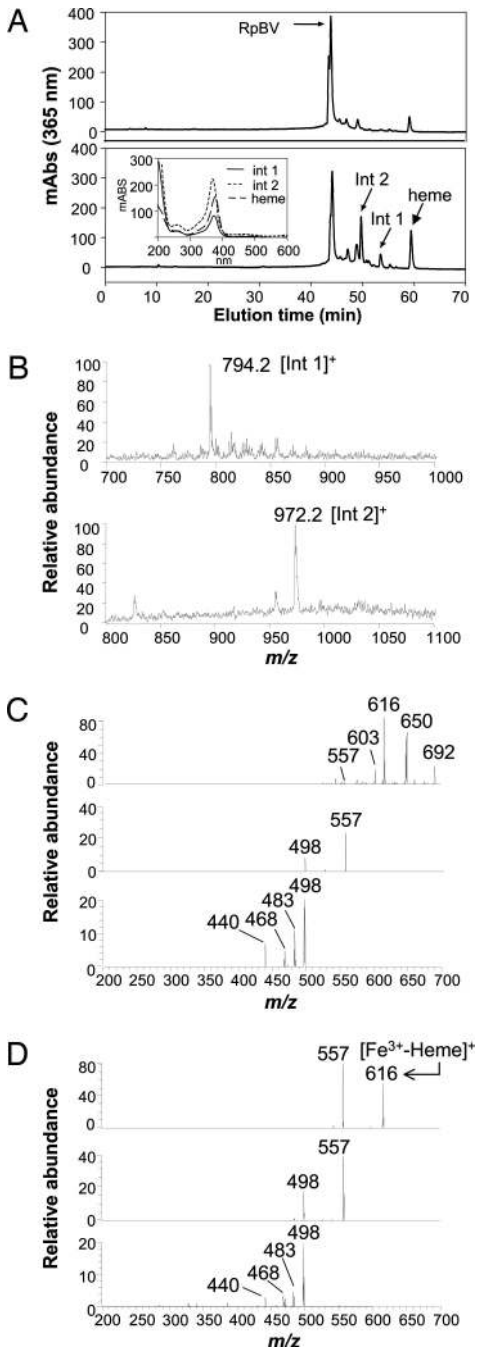

Fig. 3. Characterization of the *R. prolixus* heme-degradation pathway intermediates 1 and 2. (*A*) Reverse-phase HPLC analysis of insect heart homogenates. Insects were injected with PBS as a control (*Upper*) or coinjected with heme and SnPP IX (*Lower*). Peaks corresponding to RpBV, heme, and intermediates (Int) 1 and 2 are indicated by arrows. (*Inset*) Light-absorption spectra of Int 1 (solid line), Int 2 (dotted line), and heme (dashed line). (*B*) ESI-MS of Int 1 (*Upper*) and Int 2 (*Lower*). (*C Top*) Tandem ESI-MS of the m/z 776 ion species generated from Int 1 (shown in Fig. 5*A*). (*Middle* and *Bottom*) The fragmentation profile of the daughter ions at m/z 557 and 498, respectively. (*D*) Tandem ESI-MS of the m/z 616 ion species generated from authentic heme (*Top*). (*Middle* and *Bottom*) The fragmentation profile of the daughter ions at m/z 557 and 498, respectively.

Further evidence that intermediates 1 and 2 are part of the RpBV-production pathway was obtained by injecting insects with heme and [^{35}S]cysteine, which resulted in incorporation of label in the peaks of both intermediates (data not shown). However, the molecular masses of intermediates 1 and 2 were not consistent with the simple addition of one and two cysteine residues to heme. Instead, they are produced by attachment of one and two identical molecules of 178 Da, respectively. These molecules were shown by tandem ESI-MS to be the dipeptide cysteinylglycine (Fig. 6 *C* and *D*), a compound normally produced in mammals by intracellular metabolism of glutathione (29). Thus, we conclude that the intermediates 1 and 2 are monocysteinylglycine-heme and dicysteinylglycine-heme, respectively. The proposed assignments for the parent molecular-ion species for each intermediate and the relatively more abundant daughter-ion species are shown in Fig. 6 *C* and *D*.

Additionally, reverse-phase HPLC analysis of heart homogenates from insects previously injected with mesoheme (vinyls replaced by ethyls) did not reveal any compound with elution volume or light-absorption spectrum typical of underivatized meso-BV IX (Fig. 7, which is published as supporting information on the PNAS web site). This result strongly suggests that addition of the cysteinylglycine residues to heme vinyl groups are needed to allow efficient oxidation and cleavage of the porphyrin ring.

These findings were unexpected, because no such alterations of heme structure have been described before. Therefore, we decided to identify the intermediates downstream from intermediate 2 by injecting insects with heme and analyzing heart homogenates by liquid chromatography (LC)-MS. By this procedure, we detected two intermediates, one of m/z 939.3 and the other of m/z 882.3 (Fig. 8, which is published as supporting information on the PNAS web site). These molecules corresponded, respectively, to BV coupled with two cysteinylglycine residues (intermediate 3, Int 3) and BV bound to one cysteine and one cysteinylglycine (intermediate 4, Int 4) (Fig. 9 *C* and *D*, which is published as supporting information on the PNAS web site). Fragmentation of these molecules produced common daughter-ion species (Fig. 8 *A* and *B*), some identical to those produced by fragmentation of RpBV (m/z 686 and m/z 704) (Fig. 2*B*), thus confirming that the molecules are precursors of RpBV.

Based on these findings, we propose that, in *R. prolixus*, heme catabolism involves three distinct steps: (*i*) modification of heme by two consecutive additions of cysteinylglycine dipeptides or glutathione, in the latter case, followed by removal of the glutamic residues; (*ii*) oxidative cleavage of the porphyrin ring of dicysteinylglycine-heme to dicysteinylglycine-BV IXγ; and (*iii*) hydrolysis of the cysteine–glycine peptide bonds by a dipeptidase, releasing the end product RpBV, a dicysteinyl-BV IXγ. The proposed heme-degradation pathway is represented schematically in Fig. 4.

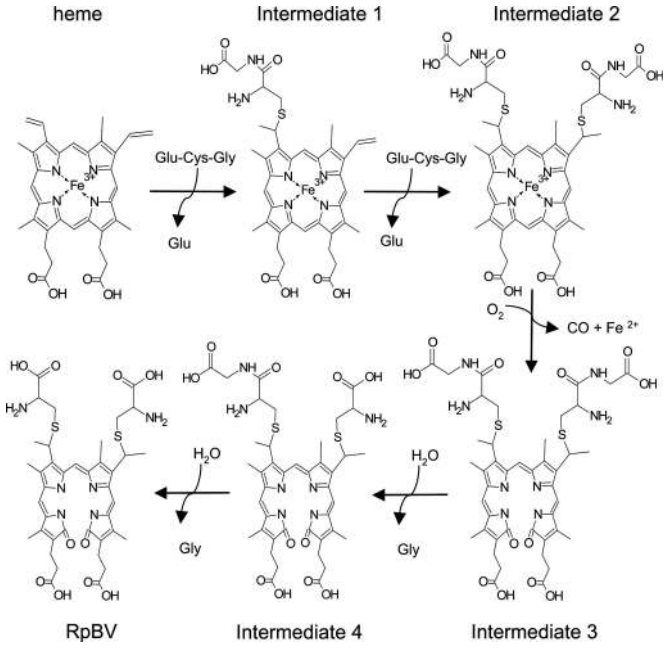

Fig. 4. The proposed heme-degradation pathway in *R. prolixus*.

Discussion

In all cases reported until now, heme breakdown is accomplished by HO, a single enzyme that produces BV IX. Here, we describe a pathway where heme is chemically modified before oxidative cleavage of the porphyrin ring, leading to accumulation of a dicysteinyl-BV IXγ as the main end product.

The first modified form of heme we found was a cysteinylglycine-heme. The most plausible explanation for the production of this compound would involve glutathione as the donor of the cysteinylglycine dipeptide. When the complete heme-modification pathway is considered, it is remarkable that exactly the same group of reactions, involving conjugation and processing of glutathione, operates during the synthesis of cysteinyl-leukotrienes from leukotriene A4 in mammalian cells (30). In smooth muscle cells, the addition of glutathione to leukotriene A4 is performed by a microsomal glutathione *S*-transferase, member of a class of enzymes known for their involvement in the detoxification of endogenous or xenobiotic compounds in many organisms (30). Cysteinylglycine-leukotrienes are then trimmed by the action of proteases, generating cysteinyl-leukotrienes.

However, because we did not find a glutathione–heme intermediate, we cannot exclude that cysteinylglycine itself may be the substrate for the initial heme modification. Alternatively, one could also speculate that a glutathione molecule may be first added to heme by a specific lyase activity, and, then, γ-glutamyl residue is removed by a γ-glutamyl-transpeptidase (29). Lyase activities are involved in the binding of the α-carbon of heme vinyl to the cysteine sulfur atom of apocytochrome C (27) and in the convalent attachment of phycobiliproteins to their bilin chromophores (31). An intrinsic lyase activity presented by apophytochromes is responsible for their α-thioether linkage to the ethylidene groups of their respective BV-derived chromophores (17) and the β-thioether linkage of BV vinyl groups to a bacteriophytochromes (28).

The biochemical and physiological significance of the addition of hydrophilic residues to heme molecules is unclear. Perhaps this could be a way to achieve the excretion of large amounts of BV, a nonhydrophilic molecule, produced after blood digestion. Similarly, in mammals, bilirubin is excreted only after conjugation to glucuronic acid. Failure in this process results in the massive accumulation of bilirubin and can lead to neurotoxic damage as observed in Crigler–Najjar syndrome (32–35). Therefore, these adaptations could represent a case of convergent evolution, resulting in the effective prevention of membrane damage and cytotoxicity by the accumulation of the hydrophobic heme-degradation products.

The production of a BV IXγ isomer indicates that *R. prolixus* expresses a HO enzyme capable of cleaving the porphyrin ring at the γ position. Recent elegant works have shown that the position of heme hydroxylation is determined by ionic interactions between heme and the HO enzyme (36–40). In addition, mutations of some specific HO-charged amino acid residues lining the active-site cavity that interact with heme propionic acid groups cause alterations of heme oxidation regiospecificity (40). In the case of RpBV production, we could hypothesize that

the presence of charged cysteine carboxyl groups in the unusual substrate, intermediate 2, may establish specific ionic interactions between this modified heme and HO, determining a γ-specific cleavage. Besides, it is feasible to speculate that *R. prolixus* HO may present particular differences in its active-site conformation that allow it to accommodate this modified heme. Thus, the *R. prolixus* system described here gives insights and could provide a unique model to better understand lesser-known aspects of the chemistry and biology of heme degradation.

Finally, production of both oxygen and nitrogen radicals as a pathogen-killing mechanism is a hallmark of innate immunity. Therefore, redox balance, the equilibrium between oxidative challenge and protective detoxification mechanisms, is a critical factor in the interaction between microorganisms that live in the gut lumen and the epithelial cells of the midgut, as shown for both mosquito-transmitted pathogens (41) and for bacterial intestinal flora of *Drosophila* (42). In the latter report, it was shown that silencing of an extracellular immune-related catalase in the midgut of *Drosophila* causes high mortality in flies after ingestion of live or even dead bacteria because of intense oxidative damage to midgut cells.

HO is well known as one of the most prominent proteins taking part in the stress response of eukaryotic cells (43). Therefore, the existence of the unique pathways described here suggests that stress-response in hematophagous animals may differ significantly from that found in other organisms.

Multiple lines of evidence clearly indicate that hematophagy has appeared independently several times during the evolution of arthropods (44), i.e., different groups of present-day hematophagous animals derive from a nonhematophagous ancestor. Thus, in the course of their evolution, several different protective mechanisms have evolved, allowing these organisms to be successfully adapted to bloodfeeding. In conclusion, our results demonstrate the existence of several activities involved in heme detoxification, used in a strategy that could possibly be shared by other hematophagous insects. Characterization of such heme-metabolizing systems and their role as a defense mechanism against heme toxicity could help in understanding the molecular basis of the adaptation to a bloodfeeding lifestyle. Moreover, this characterization could also establish an important component of the interaction between pathogens and insect hosts. In addition, such studies could lead to the discovery of interesting targets for drug-design and vector-control strategies, allowing the development of highly specific insecticides and/or manipulation of the vector's ability to transmit parasites.

Materials and Methods

Chemicals and Preparation of BV IXγ. Hemin (Fe(III) protoporphyrin IX chloride), Fe(III) mesoporphyrin IX chloride, Sn(IV)-PP IX, and BV IXα were purchased from Frontier Scientific (Logan, UT). BV IXγ, the chromophore of the *Manduca sexta* biliprotein insecticyanin was extracted from larval hemolymph (45). Hemolymph collected in cold 20 mM Tris·HCl, 100 mM NaCl buffer, pH 8.0, saturated with phenylthiourea was centrifuged at 1,000 × *g* to remove hemocytes and any precipitates. After acidification (by adding 0.2 ml of 5 N HCl and 0.2 ml of glacial acetic acid to each ml of hemolymph) BV IXγ was extracted into an equal volume of chloroform. The chloroform layer was washed three times with water and evaporated under a stream of nitrogen. To remove remaining contaminants, BV IXγ was dissolved quickly in chloroform, transferred to a fresh tube, and dried again. The BV IXγ residue was stored under nitrogen atmosphere and protected from light at −20°C. Hemin, Fe(III) mesoporphyrin IX chloride, SnPP IX, and BV stock solutions were freshly prepared in 0.1 mM NaOH or DMSO.

Insects, Treatments, and Pigment Extraction. *R. prolixus* were maintained at 28°C and 70% relative humidity. Mated female insects, fed on rabbit blood at 3-week intervals, were used in all experiments. The [^{14}C]heme *Rhodnius* heme-binding protein RHBP was obtained as described in ref. 46. Injections were performed as described in ref. 25. Dissected insect hearts were homogenized in PBS, pH 7.4, and centrifuged for 5 min at 12,000 × *g*. Supernatants were kept protected from light and stored at −20°C until use.

HPLC Fractionation. HPLC on a Shimadzu CLC-ODS C18 column (15 mm × 22 cm) was performed by using a LC-10AT device (Shimadzu, Tokyo) equipped with a diode array detector (SPD-M10A). Chromatography analysis was performed by using 5% acetonitrile with 0.05% trifluoroacetic acid (TFA) as solvent, at a flow rate of 0.4 ml/min. Before injection, samples were diluted 2 times in 5% acetonitrile with 0.05% TFA and centrifuged for 15 min at 12,000 × *g*. Ten minutes after injection of the sample, a 40-min linear acetonitrile gradient (5–80%) was applied, and the final concentration was maintained for 20 min. For identification and characterization of intermediates, heart homogenates were analyzed by nano-HPLC (Ultimate; LC Packings, Dionex, Sunnyvale, CA) by using a laboratory-made reverse-phase capillary column, assembled in a 10-cm fused silica capillary (75 μm i.d. × 360 μm o.d.; Polymicro Technologies, Phoenix, AZ) with a C18 resin (10–15 μm, 300Å; Vydac, Hesperia, CA). Chromatography conditions were as described above, except that TFA was replaced by formic acid, and the flow rate was 0.2 μl/min.

Absorption Spectroscopy. Light-absorption spectra were obtained from BV isomers and purified RpBV dissolved in methanol/HCl (95:5 vol/vol). Spectra of heme, mesoheme, and modified heme intermediates were recorded during the chromatography by the HPLC diode array detector.

ESI-MS Mass spectra were obtained in the positive ion mode by using a Finnigan LCQ-Duo ion trap mass spectrometer (Thermo Electron, San Jose, CA). Heart homogenates and BV IX stock solutions were prepared in 50% acetonitrile/0.1% formic acid. Heme stock solutions were prepared in 100% DMSO and diluted in 50% methanol immediately before use. Samples were introduced into the electrospray source by injection through a 50-μm i.d. fused silica capillary at a 5 μl/min flow rate. ESI source and capillary voltages were set at 36–46 V and 4.5 kV, respectively; the capillary temperature was 250°C. Spectra were acquired at 3 s per scan. Collision-induced fragmentation (tandem ESI-MS) of parent ions was carried out using a relative collision energy of 30–50% (1.5–2.5 eV). For the analysis of intermediates, all fractions eluted from the nano-HPLC column were subjected to tandem ESI-MS and selective ion-monitoring (for ions at m/z 794.2, 825.3, 882.3, 939.3, and 972.2), and the most abundant ion species of each fraction was subjected to tandem ESI-MS. ESI capillary voltage was set at 1.9 kV, and the temperature at 180°C. Source-induced dissociation (cone fragmentation) was achieved by applying a cone fragmentation voltage of 10 V.

***N*-Acetylation of Free Amino Groups of RpBV.** Purified BV IXγ and RpBV were resuspended in precooled 100 μl of 1M NH_4OH. After addition of 2.5 μl of acetic anhydride, samples were incubated for 10 min at 4°C. This step was repeated two times. After incubation at 25°C for 30 min, samples were dried under vacuum and resuspended in 50% acetonitrile/0.1% formic acid for ESI-MS analysis.

Methylation of Carboxyl Groups of BV IXγ and RpBV. Purified BV IXγ and RpBV were resuspended in 100 μl of NH_4OH. After addition of 100 μl of 100% methanol, samples were incubated for 1 h at 37°C. Samples were dried under vacuum and washed two times with 100 μl of 100% methanol. The precipitates were

resuspended in 100 μl of 100% methanol and incubated for 1 h at 75°C. After addition of tert-butanol (20 μl), samples were dried under vacuum and resuspended in 50% acetonitrile/0.1% formic acid for ESI-MS analysis.

Alkylation of RpBV-Free SH Groups. Purified BV IXγ and RpBV were resuspended in 50 μl of 0.6 M Tris·HCl/6 M guanidine hydrochloride. After addition of 50 μl of 4 mM DTT, samples were incubated for 45 min at 45°C under N_2 atmosphere. Fifty microliters of 0.5 M iodoacetamide were added to the reaction, and samples were incubated for 10 min at 45°C under N_2 atmosphere. Reaction was stopped by addition of 150 μl of 0.046% TFA. Samples were dried under vacuum and resuspended in 50% acetonitrile/0.1% formic acid for ESI-MS analysis.

We thank J. S. Lima, Jr., L. M. Rodrigues, H. S. L. Coelho, L. S. C. Gomes, S. J. Tadeu, and S. R. de Cassia for valuable technical assistance; N. A. Assunção for making the capillary columns; and M. Sorenson for critical reading of the paper. This work was supported by grants from the Conselho Nacional de Desenvolvimento Científico e Tecnológico, the Coordenação de Aperfeiçoamento de Pessoal de Nível Superior, the Fundação Carlos Chagas Filho de Amparo à Pesquisa do Estado do Rio de Janeiro, the Programa de Apoio a Núcleos de Excelência, and the Howard Hughes Medical Institute. C.M.M.-M. was supported by a fellowship from Fundação do Instituto Oswaldo Cruz. I.C.A. was supported by Fundação de Amparo à Pesquisa do Estado de São Paulo Grant 98/10495-5 and the Border Biomedical Research Center/Biology/University of Texas El Paso [National Institutes of Health (NIH) Grant 5G12RR008124]. B.C.D. was supported by NIH Grant GM58918.

1. Ponka, P. (1999) *Am. J. Med. Sci.* **318,** 241–256.
2. Ryter, S. W. & Tyrrel, R. M. (2000) *Free Radical Biol. Med.* **28,** 289–309.
3. Chou, A. C. & Fitch, C. D. (1980) *J. Clin. Invest.* **66,** 856–858.
4. Schmitt, T. H., Frezzati, W. A., Jr., & Schreier, S. (1993) *Arch. Biochem. Biophys.* **307,** 96–103.
5. Tenhunen R., Marver H. S. & Schmid R. D. (1969) *J. Biol. Chem.* **244,** 6388–6394.
6. Ortiz de Montellano, P. R. & Wilks, A. (2000) *Adv. Inorg. Chem.* **51,** 359–407.
7. Ortiz de Montellano, P. R. (2000) *Curr. Opin. Chem. Biol.* **4,** 221–227.
8. Yoshida, T. & Taiko Migita, C. (2000) *J. Inorg. Biochem.* **82,** 33–41.
9. Wilks, A. (2002) *Antioxid. Redox Signal.* **4,** 603–614.
10. Maines, M. D. (1997) *Annu. Rev. Pharmacol. Toxicol.* **37,** 517–554.
11. Otterbein L. E., Bach, F. H., Alan, J., Tao Lu, H., Wysk, M., Davis, R. J., Flavell, R. A. & Choi, A. M. (2000) *Nat. Med.* **6,** 422–428.
12. Brouard S., Berberat, P. O., Tobiasch, E, Seldon, M. P., Bach, F. H. & Soares, M. P. (2002) *J. Biol. Chem.* **277,** 17950–17961.
13. Stocker, R., Yamomoto, Y., McDonagh, A. F., Glazer, A. N. & Ames, B. N. (1987) *Science* **235,** 1043–1046.
14. Dore, S. & Snyder, S. H. (1999) *Ann. N.Y. Acad. Sci.* **890,** 167–172.
15. Sedlak, T. W. & Snyder, S. H. (2004) *Pediatrics* **113,** 1776–1782.
16. Stocker, R. (2004) *Antioxid. Redox Signal.* **5,** 841–849.
17. Rockwell, N. C. & Lagarias, J. C. (2006) *The Plant Cell* **18,** 4–14.
18. Kayser, H. (1985) in *Comprehensive Insect Physiology, Biochemistry and Pharmacology*, eds. Kerkut, G. A. & Gilbert, L. I. (Pergamon, Oxford), Vol. 10, pp. 367–415.
19. Dansa-Petretski, M., Ribeiro, J. M. C., Atella, G. C., Masuda, H. & Oliveira, P. L. (1995) *J. Biol. Chem.* **270,** 10893–10896.
20. Oliveira, M. F., Silva, J. R., Dansa-Petretski, M., de Souza, W., Lins, U., Braga, C. M., Masuda, H. & Oliveira, P. L. (1999) *Nature* **400,** 517.
21. Oliveira, M. F., Timm, B. L., Machado, E. A., Miranda, K., Attias, M., Silva, J. R., Dansa-Petretski, M., de Oliveira, M. A., de Souza, W., Pinhal, N. M., *et al.* (2002) *FEBS Lett.* **512,** 139–144.
22. Pascoa, V., Oliveira, P. L., Dansa-Petretski, M., Silva, J. R., Alvarenga, P. H., Jacobs-Lorena, M. & Lemos, F. J. (2002) *Insect Biochem. Mol. Biol.* **32,** 517–523.
23. Wigglesworth, V. B. (1943) *Proc. R. Soc. London B* **131,** 313–339.
24. Machado, E. A., Oliveira, P. L., Moreira, M. F., de Souza, W. & Masuda, H. (1998) *Arch. Insect Biochem. Physiol.* **39**,133–143.
25. Ratliff, M., Zhu, R., Wilks, A. & Stojiljkovic, I. (2001) *J. Bacteriol.* **183,** 6394–6403.
26. Zhang, X., Sato, M., Sasahara, M. Migita, C. & Yoshida, T. (2004) *Eur. J. Biochem.* **271,** 1713–1724.
27. Stevens, J. M., Daltrop, O., Allen, J. W. A. & Ferguson, S. J. (2004) *Acc. Chem. Res.* **37,** 999–1007.
28. Wagner, J. R., Brunzelle, J. S., Forest, K. T. & Viestra, R. D. (2005) *Nature* **438,** 325–331.
29. Tate, S. S. & Meister, A. (1981) *Mol. Cell. Biochem.* **39,** 357–368.
30. Penrose, J. F., Austen, F. K. & Lam, B. K. (1999) in: *Inflammation: Basic Principles and Clinical Correlates*, eds. Gallin, J. I. & Snyderman, R. (Lippincott Williams & Wilkins, Philadelphia), pp. 361–372.
31. Schluchter, W. M. & Glazer, A. N. (1999) in: *The Photosynthetic Prokaryotes*, eds. Peschek, G. A., Loffelhardt, W. & Schmetterer, G. (Kluwer/Plenum, New York), pp. 83–95.
32. Schmid, R. & McDonagh, A. F. (1979) *The Porphyrins*, ed. Dolphin, D. (Academic, New York.) Vol. VI, pp. 257–292.
33. Drummond, G. S. & Kappas, A. (1981) *Proc. Natl. Acad. Sci. USA.* **78,** 6466–6470.
34. Maines, M. D. (1992) *Heme Oxygenase: Clinical Applications and Functions*, ed. Maines, M. D. (CRC, Boca Raton, FL), pp 203–266.
35. McDonagh, A. (2001) *Nat. Struct. Biol.* **8,** 198–200.
36. Caignan, G. A., Deshmukh, R., Wilks, A., Zeng, Y., Huang, H. W., Moennes-Loccoz, P., Bunce, R. A., Eastman, M. A. & Rivera, M. (2002). *J. Am. Chem. Soc.* **124,** 14879–14892.
37. Friedman, J., Lad, L., Li, H., Wilks, A. & Poulos, T. L. (2004) *Biochemistry* **43,** 5239–5245.
38. Fujii, H., Zhang, X. & Yoshida, T. (2004) *J. Am. Chem. Soc.* **126,** 4466–4467.
39. Rivera, M. & Zeng, Y. (2005) *J. Inorg. Biochem.* **99,** 337–354.
40. Wang, J., Evans, J. P., Ogura, H., La Mar, G. N. & Ortiz de Montellano, P. R. (2006) *Biochemistry* **45,** 61–73.
41. Kumar, S., Christophides, G. K., Cantera, R., Charles, B., Han, Y. S., Meister, S., Dimopoulos, G., Kafatos, F. C. & Barillas-Mury, C. (2003) *Proc. Natl. Acad. Sci. USA* **100,** 14139–14144.
42. Ha, E. M., Oh, C. T., Ryu, J. H., Bae, Y. S., Kang, S. W., Jang, I. H., Brey, P. T. & Lee, W. J. (2005) *Dev. Cell* **8,** 125–132.
43. Ryter, S. W. & Choi, A. M. (2005) *Antioxid. Redox Signal.* **7,** 80–91.
44. Ribeiro, J. M. (1995) *Infect. Agents Dis.* **4,** 143–152.
45. Holden, H. M., Rupnievski, W. R., Law, J. H. & Rayment, I. (1987) *EMBO J.* **6,** 1565–1570.
46. Braz, G. R. C., Moreira, M. F., Masuda, H. & Oliveira, P. L. (2002) *Insect Biochem. Mol. Biol.* **32,** 361–367.